Encyclopedia of Systems and Control
DOI 10.1007/978-1-4471-5102-9_221-1

Vehicular Chains

Mihailo R. Jovanović*
Department of Electrical and Computer Engineering, University of Minnesota, Minneapolis, MN, USA

Abstract

Even since pioneering work of Levine and Athans and Melzer and Kuo, control of vehicular formations has been a topic of active research. In spite of its apparent simplicity, this problem poses significant engineering challenges, and it has often inspired theoretical developments. In this article, we view vehicular formations as a particular instance of dynamical systems over networks and summarize fundamental performance limitations arising from the use of local feedback in formations subject to stochastic disturbances. In topology of regular lattices, it is impossible to have coherent large formations, which behave like rigid lattices, in one and two spatial dimensions; yet this is achievable in 3D. This is a consequence of the fact that, in 1D and 2D, local feedback laws with relative position measurements are ineffective in guarding against disturbances with slow temporal variations and large spatial wavelength.

Keywords Fundamental performance limitations • Localized control • Optimal control • Relative information exchange • Spatially invariant systems • Toeplitz and circulant matrices • Vehicular formations

Introduction

Control of vehicular strings has been an active area of research for almost five decades (Levine and Athans 1966; Melzer and Kuo 1971a, b; Varaiya 1993; Swaroop and Hedrick 1996, 1999; Seiler et al. 2004; Middleton and Braslavsky 2010; Lin et al. 2012). This problem represents a special instance of more general vehicular formation problems which are encountered in the control of unmanned aerial vehicles, satellite formations, and groups of autonomous robots (Bullo et al. 2009; Mesbahi and Egerstedt 2010). Even for the simplest control objective, in which it is desired to maintain a constant cruising velocity and a constant distance between the neighboring vehicles, it has been long recognized that limited information exchange between the vehicles imposes fundamental performance limitations for control design. In particular, look-ahead strategies that rely only on relative spacing information with respect to the preceding vehicle suffer from *string instability*. This phenomenon is characterized by unfavorable amplification of disturbances downstream the vehicular string (Swaroop and Hedrick 1996, 1999; Seiler et al. 2004; Middleton and Braslavsky 2010). In order to avoid this unfavorable spatial application, it is typically required to broadcast the state of the leader to the rest of the formation.

While a precise characterization of fundamental performance limitations in the control of vehicular formations is still an open question, in this article we review recent progress in this area. We begin by highlighting performance limits that arise even in optimally controlled vehicular strings. The LQR problem for vehicular strings was originally formulated in pioneering papers by Levine and Athans (1966) and Melzer and Kuo (1971a, b). These formulations were revisited in

*E-mail: mihailo@umn.edu

Encyclopedia of Systems and Control
DOI 10.1007/978-1-4471-5102-9_221-1

Jovanović and Bamieh (2005) where it was shown that the time constant of the optimally controlled closed-loop system increases linearly with the number of vehicles. This reference also employed spatially invariant theory (Bamieh et al. 2002) to demonstrate the lack of exponential stability in the limit of an infinite number of vehicles and to explain the arbitrarily slowing rate of convergence observed in numerical studies of finite strings of increasing sizes. We then summarize a recent result that viewed vehicular strings as the 1D version of vehicular formations on regular lattices in arbitrary spatial dimensions and established fundamental performance limitations of spatially invariant localized feedback strategies with relative position measurements (Bamieh et al. 2012). It was shown that it is impossible to achieve robustness to stochastic disturbances with only localized feedback in 1D and 2D; yet this can be achieved in 3D. This is a consequence of the fact that, in 1D and 2D, local feedback laws are ineffective in guarding against disturbances with slow temporal variations and large spatial wavelength. An "accordion" type of motion experienced by these spatiotemporal modes compromises formation throughput, and it may occur even in formations that are string stable. Since the phenomenon that we describe also occurs in distributed averaging algorithms, global mean first passage time of random walks, effective resistance in electrical networks, and statistical mechanics of harmonic solids, it is relevant for a broad class of networked dynamical systems.

Optimal Control of Vehicular Strings

We next summarize a linear quadratic regulator problem for vehicular strings (Levine and Athans 1966; Melzer and Kuo 1971a, b) and demonstrate that strategies that penalize only relative position errors between neighboring vehicles yield nonuniform rates of convergence towards the desired formation (Jovanović and Bamieh 2005). In particular, the time constant of the optimally controlled closed-loop system increases linearly with the number of vehicles, and the formation loses exponential stability in the limit of infinite vehicular strings.

Optimal Control of Finite Strings

A string consisting of M identical unit mass vehicles is shown in Fig. 1a. Each vehicle is modeled as a point mass that obeys the double-integrator dynamics:

$$\ddot{x}_n = u_n, \quad n \in \{1, \ldots, M\} \tag{1}$$

where x_n is the position of the nth vehicle and u_n is the control applied on the nth vehicle. A control objective is to provide the desired constant cruising velocity $\bar{v}$ and to keep the constant distance δ between the neighboring vehicles. By introducing the absolute position and velocity error variables

$$\begin{aligned} p_n(t) &:= x_n(t) - \bar{v}t + n\delta \\ v_n(t) &:= \dot{x}_n(t) - \bar{v}, \qquad n \in \{1, \ldots, M\} \end{aligned}$$

system (1) can be brought into the state-space form (Melzer and Kuo 1971a, b):

Encyclopedia of Systems and Control
DOI 10.1007/978-1-4471-5102-9_221-1

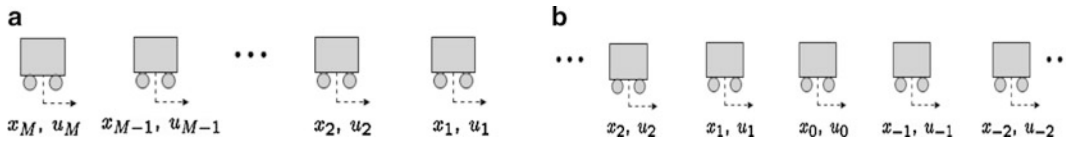

Fig. 1 Finite and infinite strings of vehicles

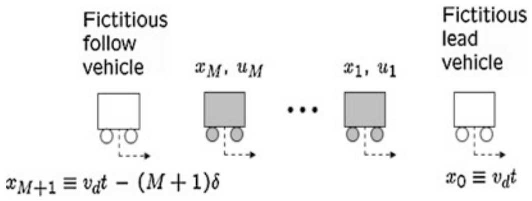

Fig. 2 Finite string with fictitious lead and follow vehicles

$$\begin{bmatrix} \dot{p} \\ \dot{v} \end{bmatrix} = \begin{bmatrix} 0 & I \\ 0 & 0 \end{bmatrix} \begin{bmatrix} p \\ v \end{bmatrix} + \begin{bmatrix} 0 \\ I \end{bmatrix} u =: A\psi + Bu \tag{2}$$

where $p := [p_1 \cdots p_M]^T$, $v := [v_1 \cdots v_M]^T$, and $u := [u_1 \cdots u_M]^T$.

Following Melzer and Kuo (1971a, b), fictitious lead and follow vehicles, respectively, indexed by 0 and $M + 1$, are added to the formation; see Fig. 2. These two vehicles are constrained to move at the desired velocity $\bar{v}$, and the relative distance between them is assumed to be equal to $(M + 1)\delta$ for all times. A quadratic performance index that penalizes control effort, relative position, and absolute velocity error variables is associated with system (2):

$$\begin{aligned} J &= \frac{1}{2}\int_0^\infty \left(\sum_{n=1}^{M+1} q_p (p_n(t) - p_{n-1}(t))^2 + \sum_{n=1}^{M} (q_v v_n^2(t) + r\, u_n^2(t)) \right) dt \\ &= \frac{1}{2}\int_0^\infty (\psi^*(t) Q \psi(t) + u^*(t) R u(t)) dt. \end{aligned} \tag{3}$$

The control problem (2) and (3) is in the standard LQR form with the state and control weights:

$$Q := \begin{bmatrix} Q_p & 0 \\ 0 & q_v I \end{bmatrix}, \quad Q_p := q_p T_M, \quad R := rI.$$

Here, T_M is an $M \times M$ symmetric Toeplitz matrix with the first row given by $[\,2\; -1\; 0 \cdots 0\,] \in \mathbb{R}^M$.

We next briefly summarize the explicit solution to the LQR problem (2) and (3) and refer the reader to Jovanović and Bamieh (2005) for additional details. By performing a spectral decomposition of the Toeplitz matrix T_M,

$$\begin{aligned} T_M &= U \Lambda_T U^*, \quad UU^* = U^*U = I \\ \Lambda_T &= \operatorname{diag}\{\lambda_1(T_M), \ldots, \lambda_M(T_M)\} \\ \lambda_n(T_M) &= 2\left(1 - \cos\tfrac{n\pi}{M+1}\right), \quad n \in \{1, \ldots, M\} \end{aligned} \tag{4}$$

the solution to the LQR algebraic Riccati equation can be represented as

$$P := \begin{bmatrix} P_1 & P_0^* \\ P_0 & P_2 \end{bmatrix}, \quad P_0 = U\Lambda_0 U^*, \quad P_2 = U\Lambda_2 U^*, \quad P_1 = U\Lambda_1 U^*.$$

Here,

$$\begin{aligned} \Lambda_0 &= \sqrt{r q_p}\, \Lambda_T^{1/2} \\ \Lambda_2 &= \sqrt{r} \left(2\sqrt{r q_p}\, \Lambda_T^{1/2} + q_v I \right)^{1/2} \\ \Lambda_1 &= \sqrt{q_p}\, \Lambda_T^{1/2} \left(2\sqrt{r q_p}\, \Lambda_T^{1/2} + q_v I \right)^{1/2} \end{aligned}$$

and the eigenvalues of the closed-loop A-matrix are determined by the solutions to the following system of the uncoupled quadratic equations:

$$\begin{aligned} s_n^2 + b_n s_n + c_n = 0, \quad & n \in \{1, \ldots, M\} \\ c_n := \left(\lambda_n(T_M) q_p / r \right)^{1/2} & \\ b_n := \left(2c_n + q_v / r \right)^{1/2}. & \end{aligned} \tag{5}$$

From the above expression, it can be shown that in large-scale formations, the least-stable eigenvalue of the closed-loop system approaches the imaginary axis at the rate that is inversely proportional to the number of vehicles. As can be seen from the PBH detectability test, this is because the pair (Q, A) gets closer to losing its detectability as the number of vehicles increases. This clearly indicates that the resulting optimal control strategy leads to closed-loop systems with arbitrarily slow decay rates as the number of vehicles increases. As summarized in section "Optimal Control of Infinite Strings," the absence of a uniform rate of convergence for a finite number of vehicles manifests itself as the absence of exponential stability in the limit of infinite vehicular strings.

Optimal Control of Infinite Strings

The LQR problem for a system of identical unit mass vehicles in an infinite string (see Fig. 1b) was originally studied in Melzer and Kuo (1971a). As summarized below, using the theory for spatially invariant linear systems (Bamieh et al. 2002), it was shown in Jovanović and Bamieh (2005) that the resulting LQR controller does not provide exponential stability of the closed-loop system due to the lack of detectability of the pair (Q, A).

The infinite dimensional equivalent of (2) is given by

$$\begin{bmatrix} \dot{p}_n \\ \dot{v}_n \end{bmatrix} = \begin{bmatrix} 0 & I \\ 0 & 0 \end{bmatrix} \begin{bmatrix} p_n \\ v_n \end{bmatrix} + \begin{bmatrix} 0 \\ I \end{bmatrix} u_n =: A_n \psi_n + B_n u_n, \quad n \in \mathbb{Z} \tag{6}$$

$$J = \frac{1}{2} \int_0^\infty \sum_{n \in \mathbb{Z}} \left(q_p (p_n(t) - p_{n-1}(t))^2 + q_v v_n^2(t) + r\, u_n^2(t) \right) dt \tag{7}$$

with q_p, q_v, and r being positive design parameters. Spatial invariance over a discrete spatial lattice $\mathbb{Z}$ can be used to establish that the solution to the LQR problem does not provide an exponentially

Encyclopedia of Systems and Control
DOI 10.1007/978-1-4471-5102-9_221-1

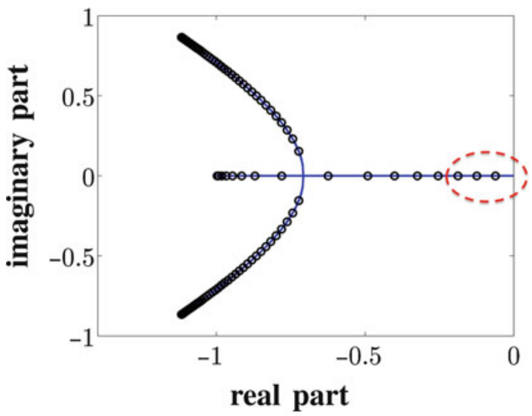

Fig. 3 The spectra of the closed-loop generators in LQR-controlled finite (*symbols*) and infinite (*solid line*) strings of vehicles with $M = 50$ and $q_p = q_v = r = 1$. The closed-loop eigenvalues of the finite string are points in the spectrum of the closed-loop infinite string. As the number of vehicles increases, the number of eigenvalues that accumulate in the vicinity of the stability boundary gets larger and larger

stabilizing feedback for system (6). In particular, the spectrum of the closed-loop generator in an LQR-controlled spatially invariant string of vehicles (6) with performance index (7) is given by the solutions to the following θ-parameterized quadratic equation:

$$\begin{aligned} s_\theta^2 + b_\theta s_\theta + c_\theta &= 0, \\ c_\theta &:= \left(2(q_p/r)(1 - \cos\theta)\right)^{1/2} \\ b_\theta &:= (2c_\theta + q_v/r)^{1/2} \end{aligned} \tag{8}$$

where $\theta \in [0, 2\pi)$ denotes the spatial wave number. By comparing (4), (5) and (8), we see that the closed-loop eigenvalues of the finite string are points in the spectrum of the closed-loop infinite string. Furthermore, from these equations it follows that as the size of the finite string increases, this set of points becomes dense in the spectrum of the infinite string closed-loop A-operator. The spectrum of the closed-loop generator, shown in Fig. 3 for $q_p = q_v = r = 1$, illustrates the absence of exponential stability.

Coherence in Large-Scale Formations

Fundamental performance limitations arising from the use of local feedback in networks subject to stochastic disturbances were recently examined in Bamieh et al. (2012). For consensus and vehicular formation control problems in topology of regular lattices, it was shown that it is impossible to guarantee robustness to stochastic exogenous disturbances in one and two spatial dimensions. Yet it was proved that this is achievable in 3D. This phenomenon is a consequence of the fact that, in 1D and 2D, local feedback laws are ineffective in guarding against disturbances with large spatial wavelength, and it has also been observed in global mean first passage time of random walks, effective resistance in electrical networks, and statistical mechanics of harmonic solids. We next briefly summarize the implications of these results for the control of vehicular formations and refer the reader to Bamieh et al. (2012) for details.

Encyclopedia of Systems and Control
DOI 10.1007/978-1-4471-5102-9_221-1

Stochastically Forced Vehicular Formations with Local Feedback

Let us consider $M := N^d$ identical vehicles arranged in a d-dimensional torus, $\mathbb{Z}_N^d$, with the double integrator dynamics:

$$\ddot{x}_n = u_n + w_n \tag{9}$$

where $n := (n_1, \ldots, n_d)$ is a multi-index with each $n_i \in \mathbb{Z}_N := \{0, \ldots, N-1\}$, u is the control input, and w is a mutually uncorrelated white stochastic forcing. Each position vector x_n is a d-dimensional vector with components $x_n := \left[x_n^1 \cdots x_n^d \right]^T$. The control objective is to have the nth vehicle follow the absolute desired trajectory $\bar{x}_n$:

$$\bar{x}_n := \bar{v}t + n\delta \Leftrightarrow \begin{bmatrix} \bar{x}_n^1 \\ \vdots \\ \bar{x}_n^d \end{bmatrix} := \begin{bmatrix} \bar{v}^1 \\ \vdots \\ \bar{v}^d \end{bmatrix} t + \begin{bmatrix} n_1 \\ \vdots \\ n_d \end{bmatrix} \delta.$$

In other words, it is desired that all vehicles move with constant heading velocity $\bar{v}$ while maintaining their respective position in a $\mathbb{Z}_N^d$ grid with spacing of δ in each dimension.

By introducing the position and velocity deviations from the desired trajectory,

$$p_n := x_n - \bar{x}_n, \quad v_n := \dot{x}_n - \bar{v}$$

and by confining our attention to static-feedback policies,

$$u(t) = -[\,K_p \;\, K_v\,] \begin{bmatrix} p(t) \\ v(t) \end{bmatrix} \tag{10}$$

equations of motion for the controlled system (9) can be brought into the state-space form

$$\begin{aligned} \begin{bmatrix} \dot{p} \\ \dot{v} \end{bmatrix} &= \begin{bmatrix} 0 & I \\ -K_p & -K_v \end{bmatrix} \begin{bmatrix} p \\ v \end{bmatrix} + \begin{bmatrix} 0 \\ I \end{bmatrix} w =: A\psi + Bw \\ z &= \quad C\psi. \end{aligned} \tag{11}$$

Here, p and v are the position and velocity vectors of all vehicles, z is the performance output, and w is the forcing vector.

An Example

In one-dimensional formations with nearest neighbor relative position and velocity measurements, the control acting on the nth vehicle is given by

$$\begin{aligned} u_n(t) = &-k_p^-(p_n(t) - p_{n-1}(t)) - k_p^+(p_n(t) - p_{n+1}(t)) \\ &-k_v^-(v_n(t) - v_{n-1}(t)) - k_v^+(v_n(t) - v_{n+1}(t)) \end{aligned} \tag{12}$$

where $k_p^{\pm}$ and $k_v^{\pm}$ are positive design parameters. For a system that evolves over a 1D lattice, the feedback gain matrices K_p and K_v are tridiagonal Toeplitz matrices implying that the

Encyclopedia of Systems and Control
DOI 10.1007/978-1-4471-5102-9_221-1

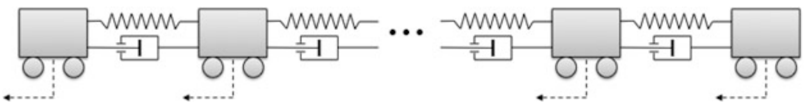

Fig. 4 Finite string of vehicles with a nearest neighbor relative position and velocity feedback

closed-loop systems have been effectively converted into a mass-spring-damper system shown in Fig. 4. Figure 5 shows the results of a stochastic simulation for the closed-loop system (11) and (12) with 100 vehicles with desired inter-vehicular spacing $\delta = 20$ and $k_p^{\pm} = k_v^{\pm} = 1$. These plots indicate the lack of formation coherence. This is only discernible when one "zooms out" to view the entire formation. The length of the formation fluctuates stochastically, but with a distinct slow temporal and long spatial wavelength signature. In contrast, the zoomed-in view in Fig. 5 shows a relatively well-regulated vehicle-to-vehicle spacing. In general, small-scale (both temporally and spatially) disturbances are well regulated, while large-scale disturbances are not. This indicates that a local feedback strategy (12) cannot regulate against large-scale disturbances.

Structural Assumptions

We now list the assumptions on the operators K_p, K_v, and C in (11) under which asymptotic scaling trends summarized in section "Scaling of Variance per Vehicle with System Size" are obtained.

- **(A1) Spatial invariance.** Operators K_p, K_v, and C in (11) are spatially invariant with respect to $\mathbb{Z}_N^d$.
- **(A2) Spatial localization.** The feedback (10) uses only local information from a neighborhood of width $2q$, where q is independent of N.
- **(A3) Reflection symmetry.** The interactions between vehicles exhibit mirror symmetry.
- **(A4) Coordinate decoupling.** For $d \geq 2$, control in each coordinate direction depends only on measurements of position and velocity error vector components in that coordinate.

While assumptions **(A3)** and **(A4)** were made to simplify calculations, assumptions **(A1)** and **(A2)** were essential for the developments in Bamieh et al. (2012).

Performance Measures

We next examine the dependence of the steady-state variance of stochastically forced system (11) on the number of vehicles. In the presence of relative position or velocity measurements, the matrix A in (11) is not necessarily Hurwitz, and the state ψ may not have finite steady-state variance. However, for connected networks, the performance output z that does not penalize the motion of the mean will have finite steady-state variance; this is because the modes of A at the origin will be unobservable from z. The steady-state variance of z,

$$V := \sum_{n \in \mathbb{Z}_N^d} \lim_{t \to \infty} \mathcal{E}\left(z_n^T(t) z_n(t)\right) \tag{13}$$

DOI 10.1007/978-1-4471-5102-9_221-1

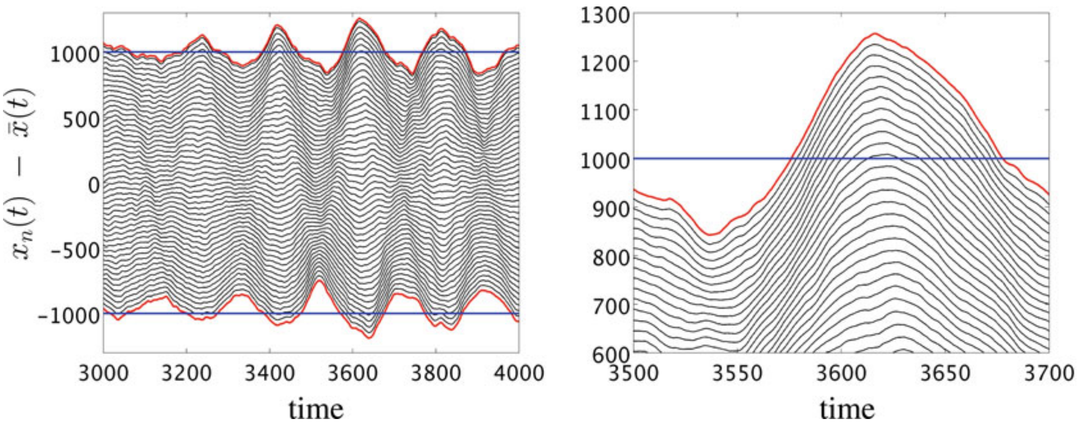

Fig. 5 Position trajectories of a stochastically forced formation with 100 vehicles controlled with nearest neighbor strategy (12). *Left plot* demonstrates accordion-like motion of the entire formation; *right plot* shows that vehicle-to-vehicle distances are relatively well regulated

is quantified by the square of the H_2 norm of the system (11) from w to z, and it can be determined from the solution of the algebraic Lyapunov equation.

We next summarize two different performance measures for stochastically forced vehicular formations.

(P1) **Local error.** This is a measure of the difference of neighboring vehicles positions from the desired spacing. In 1D, the performance output of the nth vehicle is given by

$$z_n := p_n - p_{n-1}.$$

In d-dimensions, the performance output vector contains as its components the local error in each respective dimension. Since this output involves quantities local to any vehicle within a formation, the corresponding steady-state variance is referred to as a *microscopic performance measure*, V_{micro}.

(P2) **Deviation from average.** This is a measure of the deviation of each vehicle's position error from the average of the overall position error.

$$z_n := p_n - \frac{1}{M} \sum_{j \in \mathbb{Z}_N^d} p_j. \tag{14}$$

Since this output determines deviation from average, and thereby quantities that are far apart in the network, the corresponding steady-state variance is referred to as a *macroscopic performance measure*, V_{macro}.

Scaling of Variance per Vehicle with System Size

We next summarize asymptotic bounds for both microscopic and macroscopic performance measures derived in Bamieh et al. (2012). The upper bounds result from simple feedback laws

Encyclopedia of Systems and Control
DOI 10.1007/978-1-4471-5102-9_221-1

Table 1 Asymptotic scalings of microscopic and macroscopic performance measures in terms of the total number of vehicles $M = N^d$, the spatial dimensions d, and the control effort per vehicle $U_{\max}$. Quantities listed are up to a multiplicative factor that is independent of M or $U_{\max}$:

Feedback type	V_{micro}/M	V_{macro}/M
Absolute position Absolute velocity	$\frac{1}{U_{\max}}$	$\frac{1}{U_{\max}}$
Relative position Absolute velocity	$\frac{1}{U_{\max}}$	$\frac{1}{U_{\max}} \begin{cases} M & d = 1 \\ \log(M) & d = 2 \\ 1 & d \geq 3 \end{cases}$
Relative position Relative velocity	$\frac{1}{U_{\max}^2} \begin{cases} M & d = 1 \\ \log(M) & d = 2 \\ 1 & d \geq 3 \end{cases}$	$\frac{1}{U_{\max}^2} \begin{cases} M^3 & d = 1 \\ M & d = 2 \\ M^{1/3} & d = 3 \\ \log(M) & d = 4 \\ 1 & d \geq 5 \end{cases}$

similar to the one given in (12). In the situations where either absolute position or velocity measurement are available, additional terms proportional to p_n and v_n will appear in (12). The lower bounds have been obtained for any linear static feedback control policy satisfying the structural assumptions **(A1)–(A4)** and the following constraint on control variance at each vehicle:

$$\mathcal{E}\left(u_n^T u_n\right) \leq U_{\max}. \tag{15}$$

Under this constraint, the equivalence between scaling trends of lower and upper bounds can be established. As illustrated in Table 1, the dependence of the asymptotic bounds on the number of vehicles is strongly influenced by the underlying spatial dimension d.

Since the macroscopic performance measure captures how well the formation regulates against large-scale disturbances, the scaling results presented in Table 1 demonstrate that local feedback with relative position measurements is unable to regulate against these large-scale disturbances in 1D. To the contrary, in higher spatial dimensions, local feedback can regulate against large-scale disturbances and provide formation coherence. As shown in Table 1, the "critical dimension" needed to achieve network coherence depends on the type of feedback strategy: dimension 3 for relative position and absolute velocity feedback and dimension 5 for relative position and velocity feedback.

Summary and Future Directions

For stochastically forced vehicular formations in topology of regular lattices, we have summarized fundamental performance limitations resulting from the use of local feedback. Even for formations that are string stable, local feedback is not capable of guarding against slowly varying disturbances with long spatial wavelength in 1D and 2D. The observed phenomenon also arises in distributed averaging and estimation algorithms, global mean first passage time of random walks, effective resistance in electrical networks, and statistical mechanics of harmonic solids. Since performance measures that we used to quantify robustness to disturbances are easily extensible to networks with arbitrary topology and more complex node dynamics, they can be used to evaluate performance of a broad class of networked dynamical systems in future studies.

DOI 10.1007/978-1-4471-5102-9_221-1

Cross-References

- ▸ Averaging Algorithms and Consensus
- ▸ Flocking in Networked Systems
- ▸ Networked Systems
- ▸ Oscillator Synchronization
- ▸ Steering Laws for Interacting Particles

Bibliography

Bamieh B, Paganini F, Dahleh MA (2002) Distributed control of spatially invariant systems. IEEE Trans Autom Control 47(7):1091–1107

Bamieh B, Jovanović MR, Mitra P, Patterson S (2012) Coherence in large-scale networks: dimension dependent limitations of local feedback. IEEE Trans Autom Control 57(9): 2235–2249

Bullo F, Cortés J, Martínez S (2009) Distributed control of robotic networks. Princeton University Press, Princeton

Jovanović MR, Bamieh B (2005) On the ill-posedness of certain vehicular platoon control problems. IEEE Trans Autom Control 50(9):1307–1321

Levine WS, Athans M (1966) On the optimal error regulation of a string of moving vehicles. IEEE Trans Autom Control AC-11(3):355–361

Lin F, Fardad M, Jovanović MR (2012) Optimal control of vehicular formations with nearest neighbor interactions. IEEE Trans Autom Control 57(9):2203–2218

Melzer SM, Kuo BC (1971a) Optimal regulation of systems described by a countably infinite number of objects. Automatica 7:359–366

Melzer SM, Kuo BC (1971b) A closed-form solution for the optimal error regulation of a string of moving vehicles. IEEE Trans Autom Control AC-16(1):50–52

Mesbahi M, Egerstedt M (2010) Graph theoretic methods in multiagent networks. Princeton University Press, Princeton

Middleton RH, Braslavsky JH (2010) String instability in classes of linear time invariant formation control with limited communication range. IEEE Trans Autom Control 55(7):1519–1530

Swaroop D, Hedrick JK (1996) String stability of interconnected systems. IEEE Trans Autom Control 41(2):349–357

Swaroop D, Hedrick JK (1999) Constant spacing strategies for platooning in automated highway systems. J Dyn Syst Meas Control 121(3):462–470

Seiler P, Pant A, Hedrick K (2004) Disturbance propagation in vehicle strings. IEEE Trans Autom Control 49(10):1835–1842

Varaiya P (1993) Smart cars on smart roads: problems of control. IEEE Trans Autom Control 38(2):195–207